6-2024

# SARS-CoV-2 envelope protein regulates innate immune tolerance.

Eric S. Geanes
*Children's Mercy Hospital*

Rebecca McLennan
*Children's Mercy Hospital*

Stephen H. Pierce

Heather Menden
*Children's Mercy Hospital*

Oishi Paul

*See next page for additional authors*



## Recommended Citation

Geanes ES, McLennan R, Pierce SH, et al. SARS-CoV-2 envelope protein regulates innate immune tolerance. iScience. 2024;27(6):109975. Published 2024 May 15. doi:10.1016/j.isci.2024.109975

iScience

CellPress
OPEN ACCESS

Article

# SARS-CoV-2 envelope protein regulates innate immune tolerance

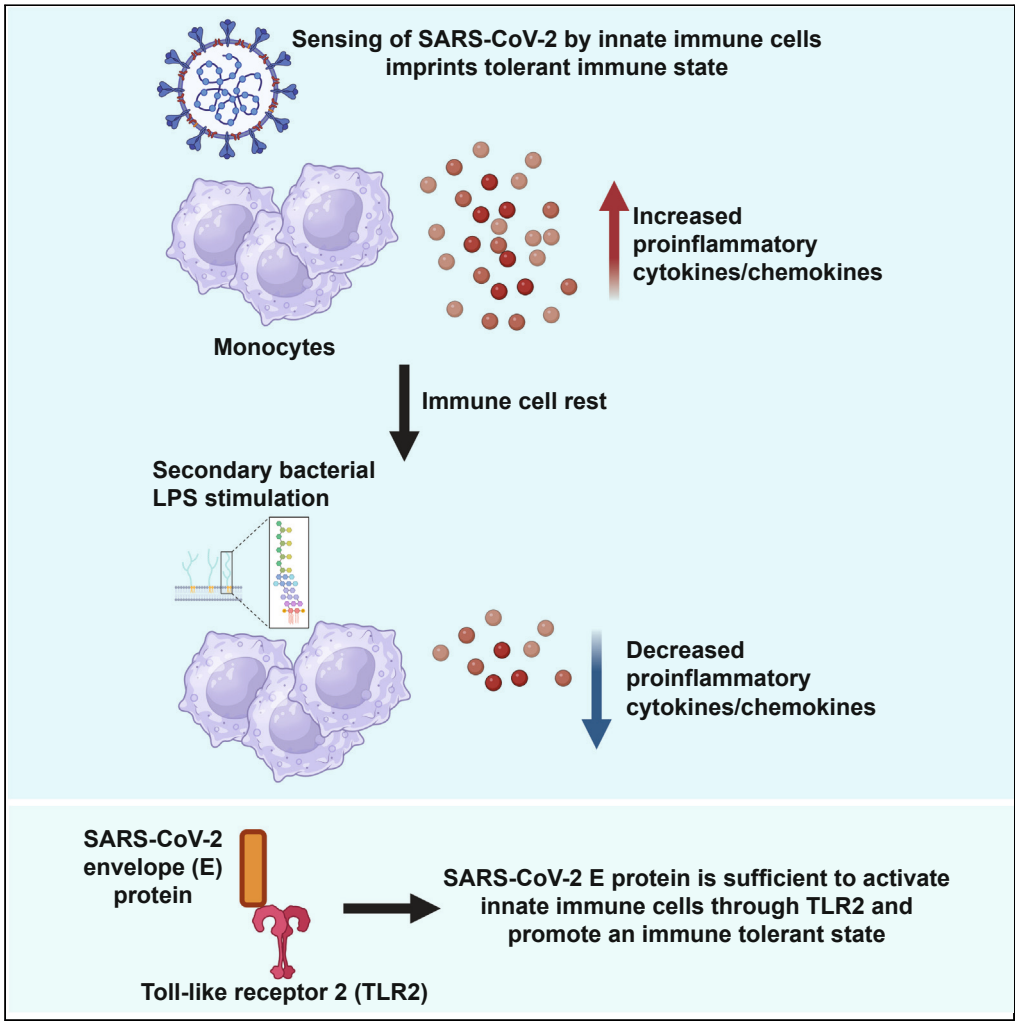


Eric S. Geanes, Rebecca McLennan, Stephen H. Pierce, Heather L. Menden, Oishi Paul, Venkatesh Sampath, Todd Bradley

tcbradley@cmh.edu

## Highlights

SARS-CoV-2 envelope (E) protein activated innate immune cells through TLR2

E protein promoted a long-term tolerant immune state after initial activation

Monocytes in this tolerant state had reduced responsiveness to secondary stimuli

E protein priming reduced lung inflammation markers to LPS in neonatal mice

Geanes et al., iScience 27, 109975
June 21, 2024 
https://doi.org/10.1016/j.isci.2024.109975

iScience

CellPress
OPEN ACCESS

Article

# SARS-CoV-2 envelope protein regulates innate immune tolerance

Eric S. Geanes,[1,6] Rebecca McLennan,[1,6] Stephen H. Pierce,[2] Heather L. Menden,[3] Oishi Paul,[1] Venkatesh Sampath,[3,4] and Todd Bradley[1,2,4,5,7,*]

## SUMMARY

**Severe COVID-19 often leads to secondary infections and sepsis that contribute to long hospital stays and mortality. However, our understanding of the precise immune mechanisms driving severe complications after SARS-CoV-2 infection remains incompletely understood. Here, we provide evidence that the SARS-CoV-2 envelope (E) protein initiates innate immune inflammation, via toll-like receptor 2 signaling, and establishes a sustained state of innate immune tolerance following initial activation. Monocytes in this tolerant state exhibit reduced responsiveness to secondary stimuli, releasing lower levels of cytokines and chemokines. Mice exposed to E protein before secondary lipopolysaccharide challenge show diminished pro-inflammatory cytokine expression in the lung, indicating that E protein drives this tolerant state *in vivo*. These findings highlight the potential of the SARS-CoV-2 E protein to induce innate immune tolerance, contributing to long-term immune dysfunction that could lead to susceptibility to subsequent infections, and uncovers therapeutic targets aimed at restoring immune function following SARS-CoV-2 infection.**

## INTRODUCTION

Prolonged immune system impairment, often triggered by strong immune activation or sepsis, heightens the vulnerability to opportunistic infections, leading to increased morbidity and mortality. Severe acute respiratory syndrome coronavirus (SARS-CoV-2) infection typically leads to mild respiratory disease, but profound acute lung injury and development of respiratory distress syndrome can lead to death in more severe cases of COVID-19.[1] Moreover, infection with even a mild clinical course of SARS-CoV-2 can lead to a variety of long-term immune-mediated and other sequalae after resolution of the viral infection.[2–7] There is urgent need to define the viral-host mechanisms of severe COVID-19 disease, and prolonged effects on immune system function, that could provide unique therapeutic targets and strategies.

Studies of COVID-19 pathology have revealed that increased levels of proinflammatory cytokines are directly associated with the pathogenesis of SARS-CoV-2.[8–11] Pro-inflammatory cytokines, such as tumor necrosis factor (TNF)-α, interleukin (IL)-1β, and interferons, are released in response to SARS-CoV-2 infection and are implicated in lung tissue damage and disease pathogenesis.[12–15] Even though numerous studies have now documented this association, the viral factors that underly dysregulated cytokine release and the impact on the long-term state of the immune system are not entirely understood. SARS-CoV-2 consists of three main structural proteins: the spike (S) glycoprotein, envelope (E) protein, and nucleocapsid (N) protein, along with several accessory proteins. The SARS-CoV-2 S protein is a surface molecule critical for virus entry into host cells and is the target of most vaccines and antibody-based therapeutics developed to block viral infection.[16–20] Although much attention has focused on the S protein to block infection, potential critical roles of the other structural proteins in the immune response and disease pathogenesis have been understudied to date. The SARS-CoV-2 N protein is responsible for viral genome packaging, and along with the genomic RNA composes the nucleocapsid, but can also be a target for antiviral and vaccine design.[21–25] The SARS-CoV-2 E protein is another viral membrane protein integral for virion assembly and budding during the coronavirus life cycle.[26–28] The E protein has high sequence conservation among SARS-CoV-2 viral variants and related coronaviruses and is also a candidate for potential preventative and therapeutic strategies.[29,30] Interestingly, the SARS-CoV-2 E protein has been shown to engage Toll-like receptor 2 (TLR2) on host cells and activate inflammatory signaling.[14,31–34] SARS-CoV-2 E protein has been shown to physically interact with TLR2 in a dose-dependent manner.[33] TLR2 was required for SARS-CoV-2 E protein induced lung inflammation, and administration of a TLR2 inhibitor, or the use of TLR2-deficient (*Tlr2*$^{-/-}$) mice protected mice from induction of inflammation.[32,34] A study of SARS-CoV-1 lacking the E protein gene

[1]Genomic Medicine Center, Children's Mercy Research Institute, Kansas City, MO, USA
[2]Department of Pathology and Laboratory Medicine, University of Kansas Medical Center, Kansas City, KS, USA
[3]Division of Neonatology, Children's Mercy Research Institute, Kansas City, MO, USA
[4]Department of Pediatrics, University of Missouri- Kansas City, Kansas City, MO, USA
[5]Department of Pediatrics, University of Kansas Medical Center, Kansas City, MO, USA
[6]These authors contributed equally
[7]Lead contact
*Correspondence: tcbradley@cmh.edu
https://doi.org/10.1016/j.isci.2024.109975

attenuated the expression of proinflammatory cytokines and increased mouse survival compared to the SARS-CoV strain that had the E protein.[31] Moreover, it has been shown that increased expression of TLRs and associated signaling pathway genes were correlated with more severe COVID-19 disease in humans, and blocking TLR2 signaling in mice protected them from COVID-19 disease.[34] Administration of recombinant SARS-CoV-2 E protein alone in mouse models was sufficient to drive this inflammation and lung tissue damage in a TLR2-dependent manner.[32,34] Thus, previous studies have demonstrated that SARS-CoV-2 E protein interacts with the innate immune system, via TLR2 signaling, to promote inflammation and lung damage. Therefore, blocking this viral-host interaction could potentially be a strategy for reducing systemic and tissue inflammation.

In addition to inflammation mediated by primary SARS-CoV-2 infection, many severe COVID-19 cases are associated with secondary infections that lead to pneumonia and sepsis.[35–37] This indicates that primary infection with SARS-CoV-2 could lead to long-term dysregulation of the innate immune system, rendering individuals more susceptible to subsequent infections and immune-mediated complications. In this study, we demonstrated that E protein (but not S or N proteins) stimulated human monocyte production of proinflammatory cytokines via TLR2 signaling, but found that this viral activation of the innate immune system imprinted a tolerant immune state that resulted in reduced response upon secondary stimulation. Induction of this tolerant state was dose dependent, and at a transcriptomic level, was caused by modulation of expression of genes regulated by NF-κB and Myc. Finally, in an *in vivo* model of secondary infection, we demonstrated that E protein exposure repressed or tolerized immune responses to lipopolysaccharide (LPS). This work unveiled how SARS-CoV-2 infection could imprint innate immune tolerance and lead to prolonged dysregulated immune responses to secondary infections.

## RESULTS

### SARS-CoV-2 E protein stimulates proinflammatory cytokine secretion in human monocytes

Prior studies have shown that SARS-CoV-2 E protein could activate a small number of proinflammatory cytokines in human peripheral blood mononuclear cells (PBMCs) or mouse-derived macrophages.[8,38] Here, we isolated monocytes from five healthy human PBMCs and determined the levels of 25 cytokines, chemokines and immune factors secreted in the cell supernatant after 24 h of stimulation with recombinant SARS-CoV-2 E, S or N proteins using a multiplexed bead-based assay (Figure 1A; Table S1). Of the 25 analytes assayed, 13 were in the quantitative range of our standards in any condition tested. E protein stimulation resulted in an average of greater than 2-fold increase of 8 of the 13 analytes compared to unstimulated control. The levels of IL-6, CCL3, CCL4, and CCL2 had the highest average increase with log2 fold-changes greater than five (Figures 1A and 1B; Table S1). Whereas the S protein had an average greater than 2-fold increase of only three analytes (CCL2, CXCL9, and CXCL10), and the N protein did not have any analytes that were increased greater than 2-fold compared to controls (Figures 1A and 1B; Table S1). These data confirmed that E protein leads to broader stimulation of proinflammatory cytokines and chemokines from human monocytes compared to the S or N protein of SARS-CoV-2.

Next, we utilized TLR2 and TLR4 reporter cell lines that consisted of HEK293 cells that expressed secreted embryonic alkaline phosphatase (SEAP) under the control of a promoter with NF-κB and AP-1 binding sites, co-transfected with either TLR2 or TLR4 to induce SEAP expression upon stimulation. Average SEAP levels measured by optical density (O.D.) for the unstimulated controls were 0.136 and 0.144 for TLR2 and TLR4 cell lines, respectively (Figure S1A). TLR2 and TLR4 HEKBlue cell lines stimulated with the respective TLR agonists as positive controls were 1.852 and 1.675 O.D., respectively (Figure S1A). We found that the recombinant E protein stimulated the TLR2 HEKBlue cell line at all five concentrations tested greater than a SEAP O.D. of 2.0, and only had minimal stimulation of the TLR4 HEKBlue cell line (O.D. of 0.589 at the highest concentration tested) (Figure 1C). The S protein did not stimulate either the TLR2 or TLR4 cell line with O.D. values at the highest concentration tested 0.149 and 0.066, respectively (Figure 1C). We also utilized the human THP-1 monocyte cell line that had integration of two inducible reporter constructs to monitor activation of the NF-κB and interferon response pathways using SEAP and luciferase reporters, respectively. We used wild-type THP-1 reporter cells as well as THP-1 cells that had a stable knock-out of the *TLR2* gene (TLR2 KO). As controls, the TLR2 agonist Heat-killed Listeria monocytogenes (HKLM) had significant activation of the wild-type cell line compared to TLR2 KO cell line, whereas the TLR4 agonist LPS activated both the wild-type and TLR2 KO THP-1 cells at equivalent levels (Figure S1B). We then stimulated the THP-1 and THP-1 TLR2 KO cell lines with recombinant SARS-CoV-2 E protein at various concentrations. We found that the E protein activated the THP-1 cells in a dose-dependent manner but did not activate the THP-1 TLR2 KO cell line above background at any concentration tested (Figure 1D). These data confirmed that SARS-CoV-2 E protein stimulated monocyte proinflammatory cytokine and chemokine secretion through TLR2 signaling. Interesting, the S protein did stimulate CCL2, CXCL9, and CXCL10 chemokines in monocytes, but most likely through a TLR2 or TLR4 independent mechanism.

### SARS-CoV-2 E protein stimulation reduces cytokine responses to secondary stimulation

To determine whether initial activation imprinted long-term dysregulation of innate immune cell function, we examined the effect of primary SARS-CoV-2 viral stimulation on monocyte function and response to secondary stimuli after rest. To do this we utilized a model of monocyte training where at day 1 monocytes were stimulated with either SARS-CoV-2 E, S, or N proteins and then allowed to rest after stimulation for five days (Figure 2A). On day 6, monocytes were restimulated with a secondary LPS stimulation (TLR4 agonist) for 24 h before the supernatant was harvested for analysis of cytokine and chemokine levels (Figure 2A). After secondary LPS stimulation, control samples (no primary stimulation) and samples initially stimulated with SARS-CoV-2 S or N proteins exhibited high levels of cytokine and chemokine stimulation, but samples initially treated with SARS-CoV-2 E protein had reduced levels of most cytokines and chemokines measured (Figure 2B; Table S2). This included pro-inflammatory IL-6 and TNF-α which have been shown to decrease during endotoxin tolerance in mice after LPS stimulation followed by cecal ligation and punction, a model of polymicrobial sepsis in mice[39]; and in human macrophages *ex vivo* after

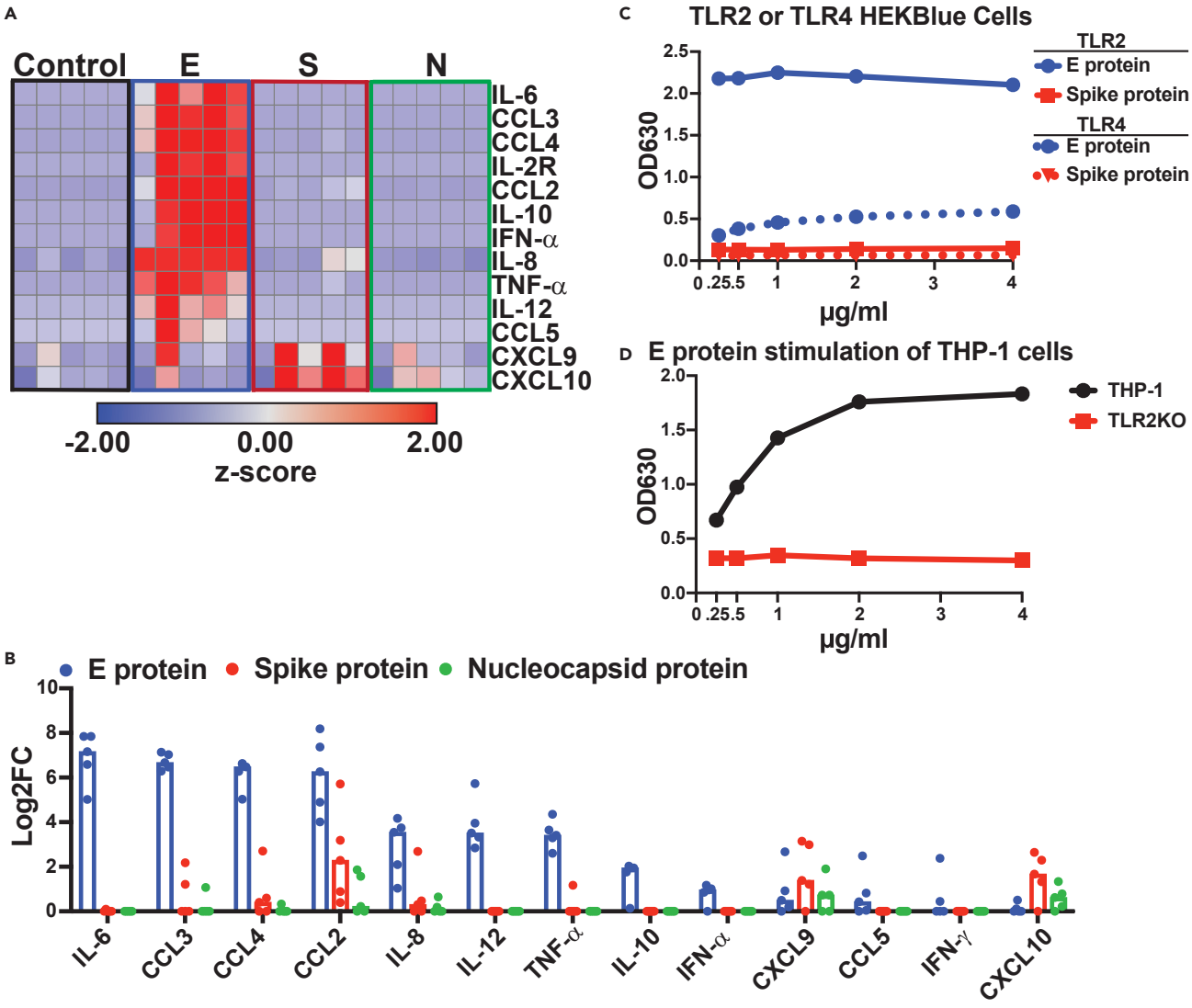


**Figure 1. SARS-CoV-2 envelope protein stimulates human monocyte cytokine secretion**

(A) Heatmap of secreted cytokine levels represented as z-scores after human monocyte stimulation with mock, envelope (E), spike (S), and nucleocapsid (N) SARS-CoV-2 viral proteins after 24 hours ($n$ = 5 individuals). Hierarchical clustering of analyte rows using 1-Pearson metric.

(B) Bar graph showing log2 fold-change of each condition compared to control (mock activated) conditions for individual analytes. Analytes ordered by descending Log2FC.

(C) HEK-Blue cell lines that express reporters for TLR2 (solid line) or TLR4 (dashed line) were stimulated with either the spike (blue) or E (red) proteins from SARS-CoV-2 at various concentrations (x-axis). Activation measured by optical density of SEAP levels in the supernatant.

(D) THP1-Dual (black line) or THP1-Dual-TLR2-KO (red line) cells stimulated with SARS-CoV-2 E protein at various concentrations (x-axis). Activation measured by optical density of SEAP levels in the supernatant.

primary and secondary stimulation with LPS.[40] Of the 13 analytes in quantitative range, monocytes stimulated with E protein before LPS exposure had significantly lower levels of 9 of the 13 cytokines and chemokines compared to control, whereas there were no significant differences in monocytes stimulated with S or N proteins for primary stimulation (Figure 2C; Table S2).

To confirm that this monocyte tolerance was due to SARS-CoV-2 E protein activation through TLR2, we utilized the THP-1 and THP-2 TLR2 KO reporter cell lines and performed initial activation with either E protein or media at day 1 followed by secondary stimulation with LPS at day 6 after rest (Figure S2A). On day 7 we measured both luciferase and SEAP levels as reporters of interferon regulatory factor (IRF) and NF-κB activation, respectively. We found that THP-1 cells that were stimulated with E protein at day 1 had a significantly reduced levels of both luciferase ($p$ = 0.003) and SEAP levels ($p$ = 0.035) after LPS secondary stimulation on day 7 compared to cells with no primary stimulation (Figure S2B). In contrast, there was no significant difference in luciferase or SEAP levels after LPS stimulation in the THP-1 TLR2 KO cells that were stimulated with the E protein or media control at day 1 (Figure S2C).

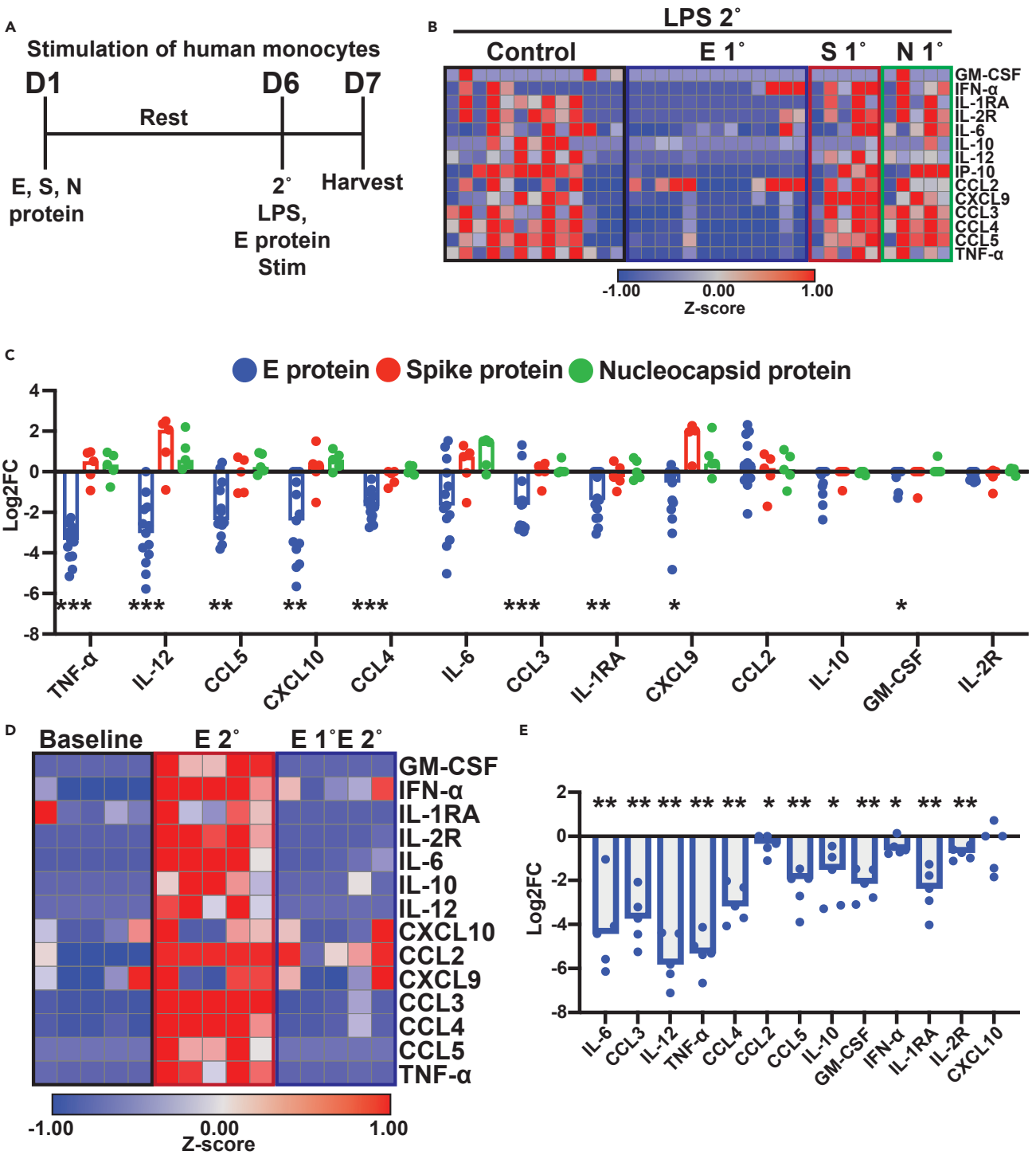


**Figure 2. SARS-CoV-2 Envelope protein tolerized monocytes to secondary stimulation**

(A) Timeline of primary and secondary stimulation of human monocytes.

(B) Heatmap of secreted cytokine levels represented as z-scores after human monocyte primary stimulation with mock ($n = 13$), envelope (E; $n = 13$), spike (S; $n = 5$), and nucleocapsid (N; $n = 5$) SARS-CoV-2 viral proteins followed by secondary stimulation with LPS. Hierarchical clustering of analyte rows using 1-Pearson metric. Control samples were not given any primary stimulation on day 1 but did receive the secondary LPS stimulation on day 6.

(C) Bar graph showing log 2-fold change of each condition compared to control (mock activated) conditions for select individual analytes measured in (B).*$p \leq 0.05$, **$p \leq 0.01$, ***$p \leq 0.001$, Paired Wilcoxon Test. Analytes ordered by descending Log2FC of E protein treated samples.

**Figure 2. *Continued***

(D) Heatmap of secreted cytokine levels presented as z-scores after human monocyte primary stimulation with envelope protein followed by secondary stimulation with envelop protein (autologous; $n = 5$). Baseline samples received no stimulations during the experiment.

(E) Bar graph showing log 2-fold change of each condition compared to control (mock activated) conditions for select individual analytes measured in (D).*$p \leq 0.05$, **$p \leq 0.01$, Paired Wilcoxon Test.

To determine if this tolerance phenotype was specific to LPS secondary stimulation, we also performed an autologous secondary stimulation with SARS-CoV-2 E protein in place of LPS (Figure 2A; Table S3). Stimulation with E protein on day 6 without primary stimulation on day 1 induced cytokine and chemokine levels similar to what was found previously with E protein stimulation (compare Figures 2D to 1A). However, when primed with E protein prior to E protein secondary stimulation, the analyte levels were similarly reduced compared to control, like LPS secondary stimulation (compare Figures 2D to 2B). Specifically, we found that 12 of the 13 analytes in quantitative range were significantly reduced after secondary E protein stimulation when primed with SARS-CoV-2 E protein first (Figure 2E; Table S3). These data demonstrated upon stimulation with SARS-CoV-2 E protein through TLR2 sensing, monocytes became tolerized and had reduced cytokine and chemokine levels upon secondary LPS or autologous E protein stimulation.

## Imprinting of monocytes by SARS-CoV-2 E protein is dose dependent

We subsequently examined how different E protein doses affected the monocyte activation state after secondary LPS stimulation. Specifically, we tested SARS-CoV-2 E protein stimulation at 1 μg/mL (used in experiments shown in Figure 2), 10 ng/mL, 1 ng/mL, and 10 pg/mL on day 1 followed by LPS stimulation on day 6. At the 1 μg/mL dose we observed the tolerance phenotype to most of the analytes as previously shown in Figure 2, but as the dose of the E protein was reduced, there was restoration of the levels of cytokines and chemokines after LPS stimulation (Figure 3A; Table S4). Interestingly, at the lowest dose there was statistically significant increases in the levels of TNF-α, IL-12, CCL3, granulocyte-macrophage colony-stimulating factor (GM-CSF), and IL-2R compared to controls, albeit, at a small magnitude of increase with a less than 1 log2 fold-change increase compared to controls (Figure 3B; Table S4). These data demonstrated that the tolerance phenotype observed in monocytes was dependent on the dose level of SARS-CoV-2 E protein primary stimulation. Specifically, high doses of E protein may be more indicative of severe COVID-19 cases, tolerizing the immune system and increasing susceptibility to other infections, whereas lower doses may shift the phenotype to more trained monocytes, reflected by higher levels of cytokines upon secondary stimulation.

## Exposure to SARS-CoV-2 E protein changes the long-term transcriptome profile of human monocytes

We then sought to determine transcriptional changes in monocytes after E protein primary stimulation and rest. We performed RNA-seq of primary human monocytes at day 6 that were stimulated at day 1 with either SARS-CoV-2 E protein or control. Compared to controls, there were 272 genes upregulated and 184 genes which had downregulated expression in response to E protein stimulation five days prior (Figure 4A; Table S5). Among the top upregulated transcripts were noncoding RNAs (*AC002480.1*, *AC022509.1*, *AC002480.2*), genes involved in metabolism (*CYP3A5* and *IDO1*), the transcription factor *OLIG2* that is involved in innate immune cell differentiation, as well as transcripts associated with proinflammatory immune responses in monocytes (*MMP3*, *CXCL5*, and *IL24*). We then performed gene set enrichment analysis (GSEA) of the differentially expressed genes to identify enriched annotated pathways. The top enriched pathways using GSEA were all involved in inflammation. The most enriched pathway were gene sets regulated by NF-κB in response to TNF (HALLMARK_TNFA_SIGNALLING_VIA_NFKB), and the third highest enriched pathway were targets known to be regulated by Myc (HALLMARK_MYC_TARGETS_V2; Figure 4B). Both NF-κB and Myc have been shown to be involved in regulating monocyte tolerance and training in response to microbial endotoxin.[41] These data demonstrated that resting monocytes stimulated with SARS-CoV-2 E protein five days prior to rest altered transcriptomes, enriching for genes regulated by NF-κB and Myc, further implicating these pathways in the regulation of the plasticity of monocyte function.

## SARS-CoV-2 E protein priming reduces inflammatory signatures in mouse lung tissue after LPS challenge

Informed by our studies in human macrophages that showed that E protein exposure suppressed the immune responses to secondary LPS stimulation *in vitro* (Figure 1), we posited that responses to LPS would be repressed in mice that had prior exposure to E protein *in vivo*. We have previously reported neonatal mouse models of inflammation and COVID-19 using systemic LPS and E protein administration and determining the effects of acute inflammation on the developing lungs.[32,42] Here, we treated neonatal mice with E protein on postnatal day 5 (P5) via intraperitoneal (i.p.) injection, followed by subsequent i.p. injection of LPS on P12 and assessed both lung inflammation and TLR signaling on P14 (Figure 5A). We noted that 9 days after E protein treatment, IL-1β and TNF-α lung expression levels were close to untreated control pups (orange; Figure 5B). LPS only treatment induced a greater than 5-fold increase in IL-1β and TNF-α cytokine expression in mice that had no prior exposure to E protein (red; Figure 5B). IL-1β and TNF-α expression was strongly suppressed on P14 in mice that were treated with E protein on P5 and then LPS on P12 (blue; Figure 5B). Interestingly, we noted that IFNα expression remain significantly elevated on P14 after E protein treatment on P5 only (orange), and LPS treatment suppressed this response (red), in contrast to other cytokines (Figure 5B).

We have shown that LPS and E protein induce TLR4 and TLR2 induced lung inflammation in this model previously.[32,42] Therefore, we investigated the effect of our treatments on canonical TLR signaling. LPS treatment induced lung phosphorylation of the NF-κB subunit, P65 (RELA) as well as the P38 Mitogen-activated protein kinase (MAPK), implying activation of TLR signaling, in mice that had no prior exposure to systemic E protein (Figures 5C and 5D). LPS-induced canonical TLR signaling activation in the lung was diminished in mice that had prior

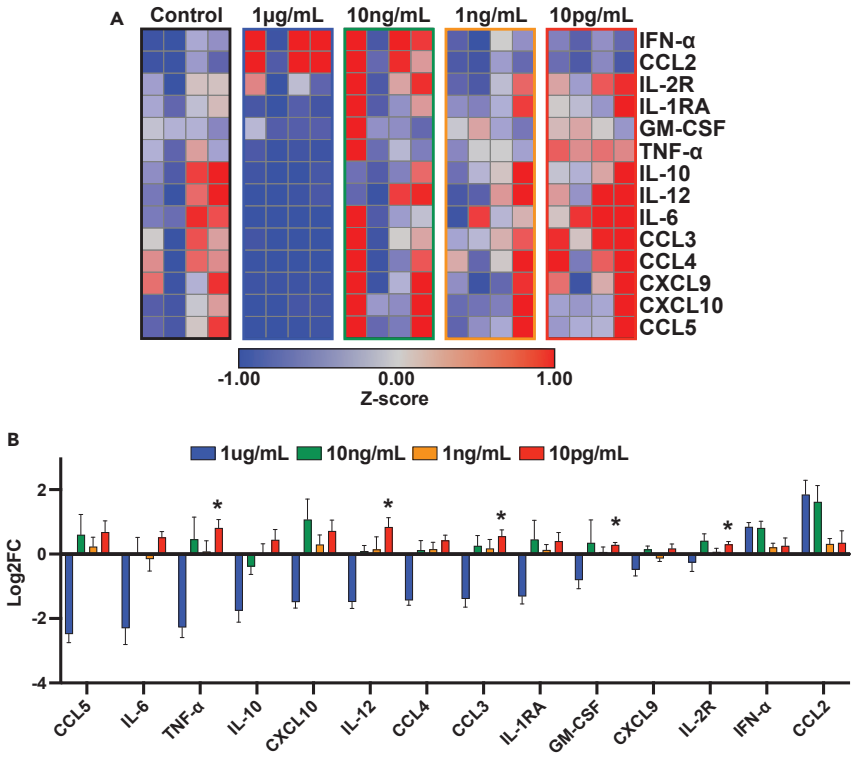


**Figure 3. SARS-CoV-2 E protein priming of monocytes is dose dependent**

(A) Heatmap of secreted cytokine levels represented as z-scores after human monocyte primary stimulation with mock ($n = 4$) or E protein stimulation at 1 µg/mL, 10 ng/mL, 1 ng/mL or 10 pg/mL dose ($n = 4$ at each dose) followed by secondary stimulation with LPS. Hierarchical clustering of analyte rows using 1-Pearson metric.

(B) Bar graph showing log 2-fold change of each condition compared to control (mock activated) conditions for individual analytes.*$p \leq 0.05$, Paired Wilcoxon Test. Error bars are standard error of the mean. Analytes ordered by descending Log2FC of highest-dose-treated samples.

exposure to E protein (Figures 5C and 5D). Importantly differences in expression of TLR2 and TLR4 were not noted in our experimental group (Figure 5D). Finally, this same pattern of expression was seen for ICAM-1, a key facilitator of neutrophil adhesion during sepsis (Figures 5C, 5D, and S3). These results suggested that prior systemic exposure to E protein attenuates LPS-induced canonical TLR signaling in a mouse model of acute lung inflammation.

## DISCUSSION

Severe COVID-19 correlates with high expression of pro-inflammatory cytokines.[8–10,14,15,43] Reducing this hyper-inflammation, initially caused by excessive activation of innate immune cells, would be an effective clinical treatment. In this study, we first showed that SARS-CoV-2 E protein is sufficient to significantly stimulate cytokine secretion from human monocytes. This stimulation was more extensive than stimulation with SARS-CoV-2 S or N viral proteins. This finding is consistent with our previous work in which we demonstrated that RNA expression of proinflammatory cytokines, such as IL-6, IL-8, and TNF-α, are induced by E protein exposure in human cell lines.[32] Additionally, here we show that E protein stimulation of monocyte cytokine secretion was via TLR2 signaling, which is consistent with recent studies demonstrating that E protein directly interacts with TLR2 and leads to increased production of pro-inflammatory cytokines.[31–34,44] In contrast to our data, some studies have concluded that the spike protein is the main component of SARS-CoV-2 for activating TLR2 or signaling in macrophages.[45–47] This could be attributed to differences in experimental design and protein administration or expression of recombinant proteins. Additionally, there has been evidence that the SARS-CoV-2 viral proteins could be associated with other mediators of inflammation that could play a role in differences observed. Future studies with mutant SARS-CoV-2 viral particles with these proteins could better determine the contribution of each of the proteins on the virion to innate immune activation. It is important to note that although our data strongly shows that E protein stimulates cytokine secretion via TLR2 signaling, this does not rule out any other modes of activation or other functional roles of the E protein during infection.

Our study adds to the mounting evidence that SARS-CoV-2 E protein impacts the immune system through TLR2 signaling and could represent an important therapeutic target for severe coronavirus disease. Three prior studies demonstrated that SARS-CoV-2 E protein activated proinflammatory cytokine expression in innate immune cells and showed that this interaction could be associated with severe disease.[32–34] These studies also showed that through genetic knock out of TLR genes, or through blockade of TLR signaling with small molecule drugs or

A

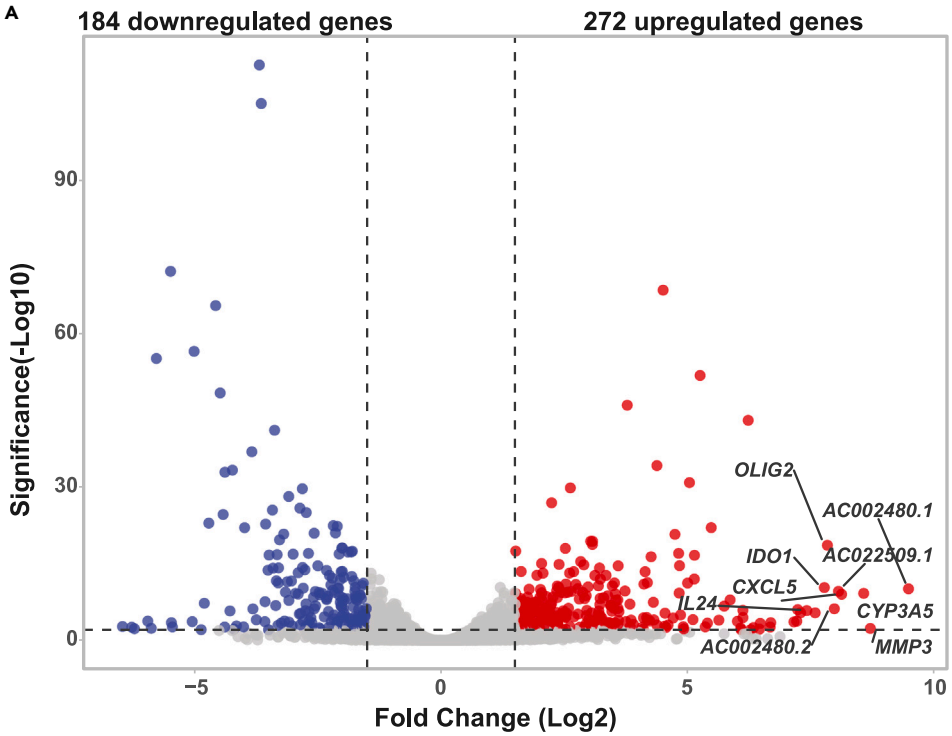


B

| NAME | SIZE | ES | NES | NOM p-val | FDR q-val | FWER p-val | RANK AT MAX |
|---|---|---|---|---|---|---|---|
| HALLMARK_TNFA_SIGNALING_VIA_NFKB | 200 | 0.693958 | 1.466253 | 0 | 0.302739 | 0.202 | 4663 |
| HALLMARK_INFLAMMATORY_RESPONSE | 200 | 0.636722 | 1.459295 | 0 | 0.176369 | 0.252 | 4377 |
| HALLMARK_MYC_TARGETS_V2 | 57 | 0.651436 | 1.371507 | 0 | 0.425747 | 0.345 | 13797 |
| HALLMARK_HYPOXIA | 200 | 0.546675 | 1.285573 | 0.102249 | 0.597089 | 0.393 | 6391 |
| HALLMARK_ALLOGRAFT_REJECTION | 196 | 0.430804 | 1.267482 | 0 | 0.582758 | 0.446 | 4802 |

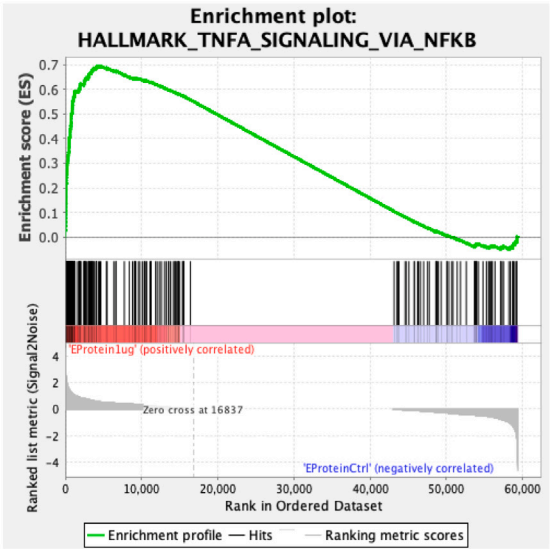


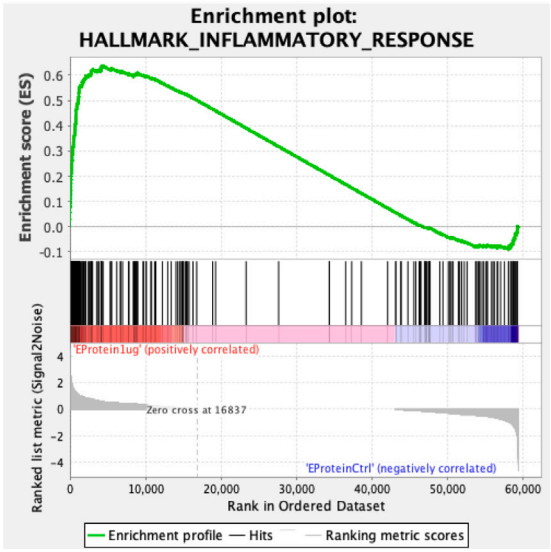


**Figure 4. SARS-CoV-2 E protein changes transcriptome of monocytes**

(A) Volcano plot of differentially expressed genes determined by RNA-seq at day 6 after either E protein ($n = 3$) or control ($n = 3$) stimulation of human monocytes. Genes upregulated by $\geq 1.5$ or downregulated by $\leq -1.5$ log2 Fold-Change in E protein stimulated compared to control are colored red or blue, respectively. Statistical significance threshold was adjusted $p$ value $\leq 0.01$.

**Figure 4. *Continued***

(B) Gene set enrichment analysis (GSEA) comparing the changed genes measured by RNA-seq enriched in the E protein stimulated monocytes compared to control. Top 5 enriched pathways and GSEA output criteria shown in the table, with the enrichment plots for the top two GSEA identified pathways enriched in the E protein stimulated monocytes.

monoclonal antibodies, that the viral E protein was specifically sensed through TLR2 signaling. Two of these studies further demonstrated physical protein-protein interactions of the E protein and TLR2 using immunoprecipitation and cellular immunofluorescence assays.[33,34] Finally, the *in vivo* relevance of the E protein-TLR2 interaction was shown when E protein administration alone induced lung inflammation in neonatal mice that was dependent on TLR2 and not TLR4 using genetic knock-outs.[32] Moreover, blockade of TLR2 with a small molecule drug reduced disease in a mouse model of COVID-19.[34] There is a lack of studies that determined the concentration of SARS-CoV-2 viral proteins in tissues after infections. However, there was a study that detected SARS-CoV-2 E protein in the blood of individuals with COVID-19 at hospital admission. They found that the levels of E protein correlated with thrombosis in this small set of COVID-19 patients.[48] The range of E protein detected in the blood was between 7.8 and 261.7 ng/mL, which is lower than the experimental concentrations that we used in our experiments. This study did not control for variables such as viral load, time after infection and other demographic differences that could impact E protein levels. In future studies, it will be interesting to determine if the level of E protein detected is associated with immune cell phenotype and function.

It was recently shown that an E protein inhibitor reduced SARS-CoV-2 release in cell culture and reduced disease severity and mortality when administered to transgenic human ACE2-expressing mice after SARS-CoV-2 infection.[49] In this same animal model of SARS-CoV-2 infection, another group showed that blocking TLR2 signaling with a TLR2 and TLR4 inhibitor (oxPAPC) reduced cytokine release and mortality.[34] This study also showed that E protein administration increased recruitment of inflammatory cells and therefore tissue damage in the lungs of wild type, but not TLR2 knock out mice.[34] In comparison, S protein did not increase inflammation in the lungs of mice when compared to controls.[34] Mice infected with a related coronavirus SARS-CoV-1 in which E protein was deleted from the virus also displayed reduced pro-inflammatory cytokine expression and lung damage.[31] Upon further examination, it was revealed that the deletion of E protein decreased NF-κB activation, and treatment of SARS-CoV-1 with NF-κB inhibitory agents also reduced lung damage and inflammation.[31]

Similarly, our own group and others have demonstrated that E protein induces inflammation and cell death *in vitro* as well as lung remodeling in a neonatal mouse model (*in vivo*), all of which is dependent on TLR2 signaling.[32,44] The animal models of SARS-CoV-2-mediated inflammation have primarily utilized adult mice. Although severe COVID-19 is more commonly associated with the elderly, individuals with preexisting health conditions, or critical illness in neonates, increased acute lung injury and mortality is observed.[50–52] This was the main driver for our group to study lung pathology after E protein-mediated inflammation in the neonatal mouse model. Systemic viremia resulting in a sepsis-like syndrome has been described in both children and adults after COVID-19,[53–55] highlighting potential long-term effects of viral infection across lifespan. The presence of various viral structural proteins in the peripheral blood has also been associated with adverse outcomes. Thus, in our neonate mouse model, we used mouse pups and administered E protein with i.p. injections to mimic viremia and to model the impact of circulatory E protein on systemic inflammation. In our prior work, we have demonstrated that i.p. E protein administration could induce lung inflammation in a TLR2-dependent manner.[32] In this study, we used this model to determine the impact of systemic E protein administration on secondary LPS stimulation. Future studies stratifying animal models or humans by age, testing different routes of E protein administration, and the effect of E protein imprinting of the immune system should be determined. These prior studies demonstrated the significant interactions between E protein, TLR2 signaling and resulting NF-κB activation in disease severity.

While multiple sources of evidence implicate SARS-CoV-2 E protein as driving acute inflammation via TLR2 sensing, it is unclear if this immune activation alters long-term responses of the innate immune system. After primary stimulation with E protein, but not S or N protein, we revealed that human monocytes become tolerized in response to a secondary stimulation. Furthermore, in a neonatal mouse challenge, we demonstrate that E protein priming suppressed lung cytokine expression and TLR signaling activation. These approaches mimic a secondary infection after an initial viral infection response to E protein exposure. The observed tolerization agrees with the observation that patients hospitalized with COVID-19 who then developed a secondary bacterial infection manifest significant immunosuppression.[56] In one study, mouse bone marrow-derived macrophages *in vitro*, as well as live mice, were transfected with E protein lentivirus and then challenged with LPS.[57] This E protein lentivirus resulted in reduced lung inflammation consistent with our data presented here.[57] Although in that study the E protein was expressed intracellularly and potentially not solely acting via TLR signaling pathways. We hypothesize that stimulation of the innate immune system by SARS-CoV-2 E protein imprints a tolerant immune state, potentially rendering individuals more susceptible to subsequent infection. This finding is significant as it highlights how prior infection history in humans could influence immune responses to current or future infections.

Tolerization of the innate immune system via TLR pathways has also been observed during and after sepsis. Sepsis, one of the leading causes of death globally, is characterized by dysregulated host response to infection, presenting both immune suppression and hyperinflammation concurrently.[58,59] One of the mechanisms of sepsis-related immune suppression during sepsis is endotoxin tolerance, which is defined as a reduced cellular response to an LPS challenge after an initial encounter with endotoxin.[60,61] In a polymicrobial sepsis model, endotoxin tolerance peaked in the first 24–48 h of sepsis, leading to, among other changes, an increase in apoptosis of immune cells.[62] This early endotoxin tolerance can lead to long-term immune paralysis, leaving individuals much more susceptible to future infections.[63] Thus, viral and bacterial imprinting of the innate immune system to alter long-term function could contribute to susceptibility to infection after many different types of infection or immune stimuli. Although the mechanisms of this immune tolerance need future attention, possible modes could include epigenetic changes, post-translational modifications of molecules downstream of the TLR pathways, and changes in adaptive immune system responses.[64,65]

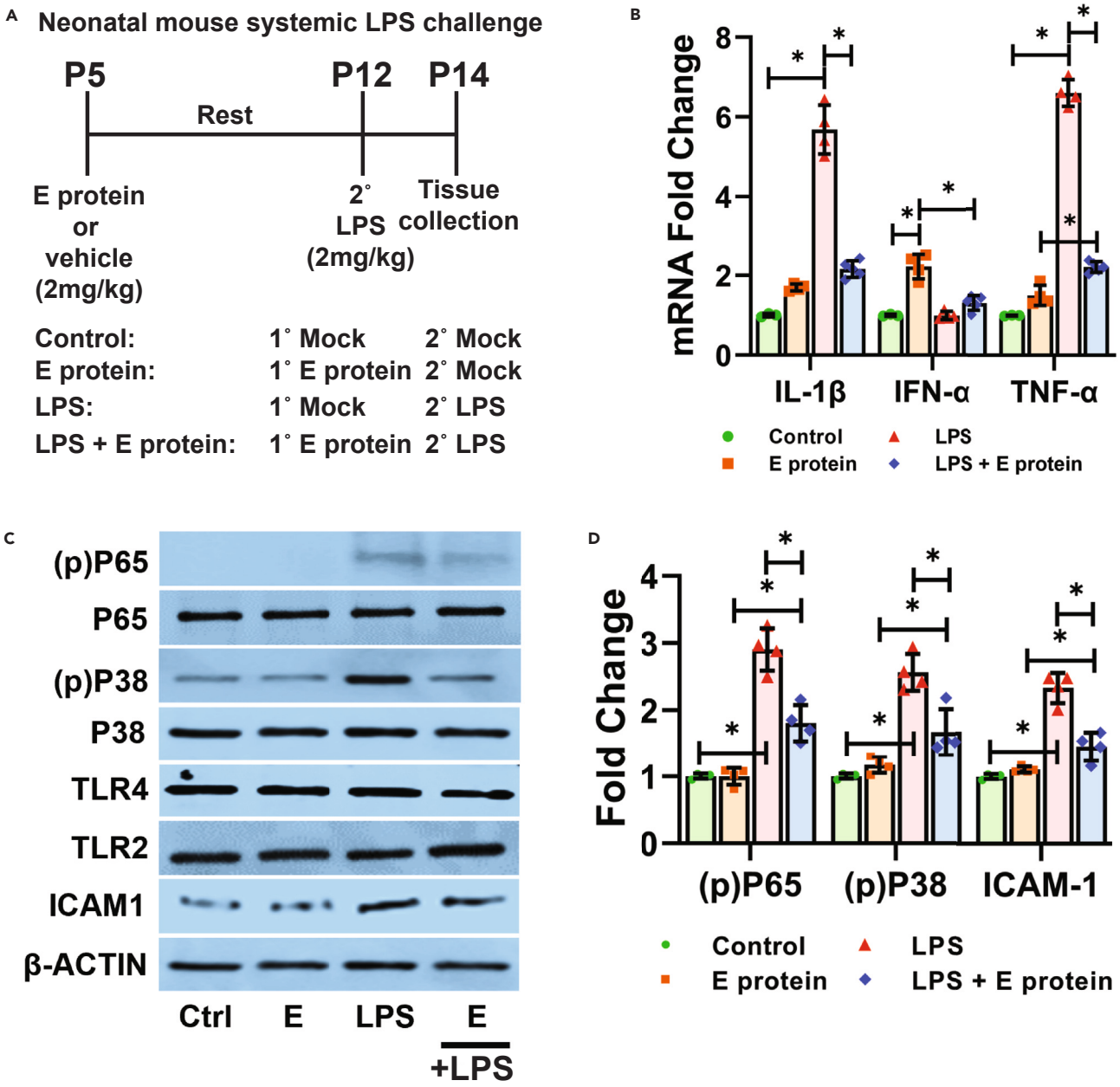


**Figure 5. Neonatal pups exposed to E protein priming have suppressed lung cytokine expression and TLR pathway activation upon challenge with systemic LPS**

(A) 5-day-old mice were injected with 2 mg/kg E protein or vehicle i.p. Subsequently, on day of life 12, mice were injected with 2 mg/kg i.p. LPS or vehicle, followed by collection of whole lung tissues on day of life 14. Whole lung homogenates were used for assays.

(B) mRNA expression of cytokine genes after various treatments. $N = 4$/group. Error bars represent standard deviations, $^*p < 0.01$.

(C and D) Protein expression of p-P65, p-P38, TLR2, and TLR4 after different treatments with densitometry quantification shown. $N = 4$/group. Error bars represent standard deviations, $^*p < 0.05$, one-way ANOVA with Bonferroni correction.

Here, we used RNA-seq of monocytes to gain insights into potential regulation of this tolerance and discovered altered transcriptomes, enriching for genes regulated by NF-κB and Myc pathways. Consistent with our findings, NF-κB activation has been shown to increase in response to E protein exposure, with very little activation in response to S or N proteins.[38] NF-κB has also been shown to play a pivotal role in regulating macrophage responsiveness[66–68] and tolerance, including perturbations during severe COVID-19.[41] Myc is a key transcription regulator that is associated with cell growth and survival, and has also been shown to play a role in macrophage activation.[69] Interestingly, the SARS-CoV-2 accessory protein Orf7b was shown to contribute to lung injury via Myc-mediated cell death.[70] These data identify key

pathways to be further explored to understand the mechanisms of SARS-CoV-2 E protein-mediated innate immune cell tolerance and identify potential targets for reversing this immune cell state.

Our data demonstrated that exposure to SARS-CoV-2 E protein, but not S and N proteins, induced significant stimulation of pro-inflammatory cytokines, imprinting a state of innate immune tolerance, which is critical for the response to secondary stimuli or infection. While we identify that the E protein more robustly signals through TLR2 compared to other viral proteins, studies that determine the effect of the viral proteins in combination could shed further insight on viral mechanisms of immune tolerance. Future studies will be required to determine if reversing this tolerant state improves resistance to secondary infection or would result in enhanced tissue damage. Therapeutic targeting of SARS-CoV-2 E protein could block inflammation early but also prevent the establishment of the innate immune tolerance state we observed. Interestingly, SARS-CoV-2, viral variants of concern, and other related coronavirus E proteins are highly similar at the amino acid sequence level[30] and therefore is a conserved target for therapeutic strategies with broader future applications. Taken together, SARS-CoV-2 E protein contributes to the early release of inflammatory cytokines and can imprint longer-term dysfunction of the innate immune system. Targeting E protein could represent an innovative strategy at reducing inflammation driven by SARS-CoV-2 infection that results in severe disease outcomes.

### Limitations of the study

Our study utilized recombinantly expressed SARS-CoV-2 viral proteins and the effect of E protein on immune imprinting could be affected by native structure on the virion as well as the amount of E protein that is present during *in vivo* viral infection. Our study was limited in determining the impact of age, sex, and other demographic and clinical parameters on the magnitude and duration of innate immune cell activation and tolerance by SARS-CoV-2. Finally, our study focused mainly on the monocyte/macrophage lineages of the innate immune system, but the effects of SARS-CoV-2 viral proteins on the activation and phenotype of other innate and adaptive immune cells should be further studied.

## STAR★METHODS

Detailed methods are provided in the online version of this paper and include the following:

- KEY RESOURCES TABLE
- RESOURCE AVAILABILITY
  - Lead contact
  - Materials availability
  - Data and code availability
- EXPERIMENTAL MODEL AND STUDY PARTICIPANT DETAILS
  - Human subjects
  - Mice
- METHOD DETAILS
  - Monocyte isolation and culture
  - Luminex multiplexed cytokine and chemokine measurements
  - SARS-CoV-2 E and S protein stimulation of TLR2 and TLR4 overexpressing HEK cells
  - SARS-CoV-2 E protein stimulation of THP-1 and THP-1 TLR2 knockout cells
  - RNA-sequencing of human monocytes
  - Mouse immunization with SARS-CoV-2 E protein
  - Quantification of mRNA expression using real-time PCR
  - Immunoblotting for quantifying changes in protein expression
- QUANTIFICATION AND STATISTICAL ANALYSIS

## SUPPLEMENTAL INFORMATION

Supplemental information can be found online at https://doi.org/10.1016/j.isci.2024.109975.

## ACKNOWLEDGMENTS

We acknowledge the CMRI Genomic Medicine sequencing core for assistance with RNA-seq.

This research was supported by funding from the Children's Mercy Research Institute, Children's Mercy Kansas City. H.L.M. and V.S. were supported in part by National Institutes of Health 1R01 DK117296-05 and 1R01 HL162937-01 awards.

## AUTHOR CONTRIBUTIONS

T.B. conceived and designed the study. E.S.G., S.H.P., O.P., and H.L.M. performed cellular and animal experimentation. T.B. and H.L.M. performed associated experimental data analysis. V.S. and T.B. interpreted the data. R.M. and T.B. wrote the manuscript, and all authors comments on the manuscript.

## DECLARATION OF INTERESTS

The authors declare no competing interests.

Received: November 28, 2023
Revised: March 1, 2024
Accepted: May 10, 2024
Published: May 15, 2024

## REFERENCES

1. Machhi, J., Herskovitz, J., Senan, A.M., Dutta, D., Nath, B., Oleynikov, M.D., Blomberg, W.R., Meigs, D.D., Hasan, M., Patel, M., et al. (2020). The Natural History, Pathobiology, and Clinical Manifestations of SARS-CoV-2 Infections. J. Neuroimmune Pharmacol. *15*, 359–386. https://doi.org/10.1007/s11481-020-09944-5.
2. Altmann, D.M., Whettlock, E.M., Liu, S., Arachchillage, D.J., and Boyton, R.J. (2023). The immunology of long COVID. Nat. Rev. Immunol. *23*, 618–634. https://doi.org/10.1038/s41577-023-00904-7.
3. Callard, F., and Perego, E. (2021). How and why patients made Long Covid. Soc. Sci. Med. *268*, 113426. https://doi.org/10.1016/j.socscimed.2020.113426.
4. Magnusson, K., Kristoffersen, D.T., Dell'Isola, A., Kiadaliri, A., Turkiewicz, A., Runhaar, J., Bierma-Zeinstra, S., Englund, M., Magnus, P.M., and Kinge, J.M. (2022). Post-covid medical complaints following infection with SARS-CoV-2 Omicron vs Delta variants. Nat. Commun. *13*, 7363. https://doi.org/10.1038/s41467-022-35240-2.
5. Michelen, M., Manoharan, L., Elkheir, N., Cheng, V., Dagens, A., Hastie, C., O'Hara, M., Suett, J., Dahmash, D., Bugaeva, P., et al. (2021). Characterising long COVID: a living systematic review. BMJ Glob. Health *6*, e005427. https://doi.org/10.1136/bmjgh-2021-005427.
6. Davis, H.E., McCorkell, L., Vogel, J.M., and Topol, E.J. (2023). Long COVID: major findings, mechanisms and recommendations. Nat. Rev. Microbiol. *21*, 133–146. https://doi.org/10.1038/s41579-022-00846-2.
7. Davis, H.E., Assaf, G.S., McCorkell, L., Wei, H., Low, R.J., Re'em, Y., Redfield, S., Austin, J.P., and Akrami, A. (2021). Characterizing long COVID in an international cohort: 7 months of symptoms and their impact. EClinicalMedicine *38*, 101019. https://doi.org/10.1016/j.eclinm.2021.101019.
8. McElvaney, O.J., McEvoy, N.L., McElvaney, O.F., Carroll, T.P., Murphy, M.P., Dunlea, D.M., Ní Choileáin, O., Clarke, J., O'Connor, E., Hogan, G., et al. (2020). Characterization of the Inflammatory Response to Severe COVID-19 Illness. Am. J. Respir. Crit. Care Med. *202*, 812–821. https://doi.org/10.1164/rccm.202005-1583OC.
9. Vabret, N., Britton, G.J., Gruber, C., Hegde, S., Kim, J., Kuksin, M., Levantovsky, R., Malle, L., Moreira, A., Park, M.D., et al. (2020). Immunology of COVID-19: Current State of the Science. Immunity *52*, 910–941. https://doi.org/10.1016/j.immuni.2020.05.002.
10. Fajgenbaum, D.C., and June, C.H. (2020). Cytokine Storm. N. Engl. J. Med. *383*, 2255–2273. https://doi.org/10.1056/NEJMra2026131.
11. Ye, Q., Wang, B., and Mao, J. (2020). The pathogenesis and treatment of the ;Cytokine Storm' in COVID-19. J. Infect. *80*, 607–613. https://doi.org/10.1016/j.jinf.2020.03.037.
12. Lucas, C., Wong, P., Klein, J., Castro, T.B.R., Silva, J., Sundaram, M., Ellingson, M.K., Mao, T., Oh, J.E., Israelow, B., et al. (2020). Longitudinal analyses reveal immunological misfiring in severe COVID-19. Nature *584*, 463–469. https://doi.org/10.1038/s41586-020-2588-y.
13. Karki, R., Sharma, B.R., Tuladhar, S., Williams, E.P., Zalduondo, L., Samir, P., Zheng, M., Sundaram, B., Banoth, B., Malireddi, R.K.S., et al. (2021). Synergism of TNF-alpha and IFN-gamma Triggers Inflammatory Cell Death, Tissue Damage, and Mortality in SARS-CoV-2 Infection and Cytokine Shock Syndromes. Cell *184*, 149–168.e17. https://doi.org/10.1016/j.cell.2020.11.025.
14. Barnett, K.C., Xie, Y., Asakura, T., Song, D., Liang, K., Taft-Benz, S.A., Guo, H., Yang, S., Okuda, K., Gilmore, R.C., et al. (2023). An epithelial-immune circuit amplifies inflammasome and IL-6 responses to SARS-CoV-2. Cell Host Microbe *31*, 243–259.e6. https://doi.org/10.1016/j.chom.2022.12.005.
15. Mulchandani, R., Lyngdoh, T., and Kakkar, A.K. (2021). Deciphering the COVID-19 cytokine storm: Systematic review and meta-analysis. Eur. J. Clin. Invest. *51*, e13429. https://doi.org/10.1111/eci.13429.
16. Piccoli, L., Park, Y.J., Tortorici, M.A., Czudnochowski, N., Walls, A.C., Beltramello, M., Silacci-Fregni, C., Pinto, D., Rosen, L.E., Bowen, J.E., et al. (2020). Mapping Neutralizing and Immunodominant Sites on the SARS-CoV-2 Spike Receptor-Binding Domain by Structure-Guided High-Resolution Serology. Cell *183*, 1024–1042.e21. https://doi.org/10.1016/j.cell.2020.09.037.
17. Toussi, S.S., Hammond, J.L., Gerstenberger, B.S., and Anderson, A.S. (2023). Therapeutics for COVID-19. Nat. Microbiol. *8*, 771–786. https://doi.org/10.1038/s41564-023-01356-4.
18. Wang, Z., Schmidt, F., Weisblum, Y., Muecksch, F., Barnes, C.O., Finkin, S., Schaefer-Babajew, D., Cipolla, M., Gaebler, C., Lieberman, J.A., et al. (2021). mRNA vaccine-elicited antibodies to SARS-CoV-2 and circulating variants. Preprint at bioRxiv. https://doi.org/10.1101/2021.01.15.426911.
19. Huang, Y., Yang, C., Xu, X.F., Xu, W., and Liu, S.W. (2020). Structural and functional properties of SARS-CoV-2 spike protein: potential antivirus drug development for COVID-19. Acta Pharmacol. Sin. *41*, 1141–1149. https://doi.org/10.1038/s41401-020-0485-4.
20. Letko, M., Marzi, A., and Munster, V. (2020). Functional assessment of cell entry and receptor usage for SARS-CoV-2 and other lineage B betacoronaviruses. Nat. Microbiol. *5*, 562–569. https://doi.org/10.1038/s41564-020-0688-y.
21. Masters, P.S. (2019). Coronavirus genomic RNA packaging. Virology *537*, 198–207. https://doi.org/10.1016/j.virol.2019.08.031.
22. Cubuk, J., Alston, J.J., Incicco, J.J., Singh, S., Stuchell-Brereton, M.D., Ward, M.D., Zimmerman, M.I., Vithani, N., Griffith, D., Wagoner, J.A., et al. (2021). The SARS-CoV-2 nucleocapsid protein is dynamic, disordered, and phase separates with RNA. Nat. Commun. *12*, 1936. https://doi.org/10.1038/s41467-021-21953-3.
23. Bai, Z., Cao, Y., Liu, W., and Li, J. (2021). The SARS-CoV-2 Nucleocapsid Protein and Its Role in Viral Structure, Biological Functions, and a Potential Target for Drug or Vaccine Mitigation. Viruses *13*, 1115. https://doi.org/10.3390/v13061115.
24. Oronsky, B., Larson, C., Caroen, S., Hedjran, F., Sanchez, A., Prokopenko, E., and Reid, T. (2022). Nucleocapsid as a next-generation COVID-19 vaccine candidate. Int. J. Infect. Dis. *122*, 529–530. https://doi.org/10.1016/j.ijid.2022.06.046.
25. Royster, A., Ren, S., Ma, Y., Pintado, M., Kahng, E., Rowan, S., Mir, S., and Mir, M. (2023). SARS-CoV-2 Nucleocapsid Protein Is a Potential Therapeutic Target for Anticoronavirus Drug Discovery. Microbiol. Spectr. *11*, e0118623. https://doi.org/10.1128/spectrum.01186-23.
26. Kuo, L., Hurst, K.R., and Masters, P.S. (2007). Exceptional flexibility in the sequence requirements for coronavirus small envelope protein function. J. Virol. *81*, 2249–2262. https://doi.org/10.1128/JVI.01577-06.
27. Schoeman, D., and Fielding, B.C. (2019). Coronavirus envelope protein: current knowledge. Virol. J. *16*, 69. https://doi.org/10.1186/s12985-019-1182-0.
28. Siu, Y.L., Teoh, K.T., Lo, J., Chan, C.M., Kien, F., Escriou, N., Tsao, S.W., Nicholls, J.M., Altmeyer, R., Peiris, J.S.M., et al. (2008). The M, E, and N structural proteins of the severe acute respiratory syndrome coronavirus are required for efficient assembly, trafficking, and release of virus-like particles. J. Virol. *82*, 11318–11330. https://doi.org/10.1128/JVI.01052-08.
29. Sarkar, M., and Saha, S. (2020). Structural insight into the role of novel SARS-CoV-2 E protein: A potential target for vaccine development and other therapeutic strategies. PLoS One *15*, e0237300. https://doi.org/10.1371/journal.pone.0237300.
30. Grifoni, A., Sidney, J., Zhang, Y., Scheuermann, R.H., Peters, B., and Sette, A. (2020). A Sequence Homology and Bioinformatic Approach Can Predict Candidate Targets for Immune Responses to SARS-CoV-2. Cell Host Microbe *27*, 671–680.e2. https://doi.org/10.1016/j.chom.2020.03.002.
31. DeDiego, M.L., Nieto-Torres, J.L., Regla-Nava, J.A., Jimenez-Guardeño, J.M., Fernandez-Delgado, R., Fett, C.,

Castaño-Rodriguez, C., Perlman, S., and Enjuanes, L. (2014). Inhibition of NF-kappaB-mediated inflammation in severe acute respiratory syndrome coronavirus-infected mice increases survival. J. Virol. *88*, 913–924. https://doi.org/10.1128/JVI.02576-13.

32. Menden, H.L., Mabry, S.M., Venkatraman, A., Xia, S., DeFranco, D.B., Yu, W., and Sampath, V. (2023). The SARS-CoV-2 E protein induces Toll-like receptor 2-mediated neonatal lung injury in a model of COVID-19 viremia that is rescued by the glucocorticoid ciclesonide. Am. J. Physiol. Lung Cell Mol. Physiol. *324*, L722–L736. https://doi.org/10.1152/ajplung.00410.2022.
33. Planes, R., Bert, J.B., Tairi, S., BenMohamed, L., and Bahraoui, E. (2022). SARS-CoV-2 Envelope (E) Protein Binds and Activates TLR2 Pathway: A Novel Molecular Target for COVID-19 Interventions. Viruses *14*, 999. https://doi.org/10.3390/v14050999.
34. Zheng, M., Karki, R., Williams, E.P., Yang, D., Fitzpatrick, E., Vogel, P., Jonsson, C.B., and Kanneganti, T.D. (2021). TLR2 senses the SARS-CoV-2 envelope protein to produce inflammatory cytokines. Nat. Immunol. *22*, 829–838. https://doi.org/10.1038/s41590-021-00937-x.
35. Ripa, M., Galli, L., Poli, A., Oltolini, C., Spagnuolo, V., Mastrangelo, A., Muccini, C., Monti, G., De Luca, G., Landoni, G., et al. (2021). Secondary infections in patients hospitalized with COVID-19: incidence and predictive factors. Clin. Microbiol. Infect. *27*, 451–457. https://doi.org/10.1016/j.cmi.2020.10.021.
36. Karakike, E., Giamarellos-Bourboulis, E.J., Kyprianou, M., Fleischmann-Struzek, C., Pletz, M.W., Netea, M.G., Reinhart, K., and Kyriazopoulou, E. (2021). Coronavirus Disease 2019 as Cause of Viral Sepsis: A Systematic Review and Meta-Analysis. Crit. Care Med. *49*, 2042–2057. https://doi.org/10.1097/CCM.0000000000005195.
37. Cohen, R., Babushkin, F., Finn, T., Geller, K., Alexander, H., Datnow, C., Uda, M., Shapiro, M., Paikin, S., and Lellouche, J. (2021). High Rates of Bacterial Pulmonary Co-Infections and Superinfections Identified by Multiplex PCR among Critically Ill COVID-19 Patients. Microorganisms *9*, 2483. https://doi.org/10.3390/microorganisms9122483.
38. Anand, G., Perry, A.M., Cummings, C.L., St Raymond, E., Clemens, R.A., and Steed, A.L. (2021). Surface Proteins of SARS-CoV-2 Drive Airway Epithelial Cells to Induce IFN-Dependent Inflammation. J. Immunol. *206*, 3000–3009. https://doi.org/10.4049/jimmunol.2001407.
39. Wheeler, D.S., Lahni, P.M., Denenberg, A.G., Poynter, S.E., Wong, H.R., Cook, J.A., and Zingarelli, B. (2008). Induction of endotoxin tolerance enhances bacterial clearance and survival in murine polymicrobial sepsis. Shock *30*, 267–273. https://doi.org/10.1097/shk.0b013e318162c190.
40. Kox, M., de Kleijn, S., Pompe, J.C., Ramakers, B.P., Netea, M.G., van der Hoeven, J.G., Hoedemaekers, C.W., and Pickkers, P. (2011). Differential ex vivo and in vivo endotoxin tolerance kinetics following human endotoxemia. Crit. Care Med. *39*, 1866–1870. https://doi.org/10.1097/CCM.0b013e3182190d5d.
41. Dorneles, G.P., Teixeira, P.C., Peres, A., Rodrigues Júnior, L.C., da Fonseca, S.G., Monteiro, M.C., Eller, S., Oliveira, T.F., Wendland, E.M., and Romão, P.R.T. (2023). Endotoxin tolerance and low activation of TLR-4/NF-kappaB axis in monocytes of COVID-19 patients. J. Mol. Med. *101*, 183–195. https://doi.org/10.1007/s00109-023-02283-x.
42. Menden, H.L., Xia, S., Mabry, S.M., Navarro, A., Nyp, M.F., and Sampath, V. (2016). Nicotinamide Adenine Dinucleotide Phosphate Oxidase 2 Regulates LPS-Induced Inflammation and Alveolar Remodeling in the Developing Lung. Am. J. Respir. Cell Mol. Biol. *55*, 767–778. https://doi.org/10.1165/rcmb.2016-0006OC.
43. Del Valle, D.M., Kim-Schulze, S., Huang, H.H., Beckmann, N.D., Nirenberg, S., Wang, B., Lavin, Y., Swartz, T.H., Madduri, D., Stock, A., et al. (2020). An inflammatory cytokine signature predicts COVID-19 severity and survival. Nat. Med. *26*, 1636–1643. https://doi.org/10.1038/s41591-020-1051-9.
44. Xia, B., Shen, X., He, Y., Pan, X., Liu, F.L., Wang, Y., Yang, F., Fang, S., Wu, Y., Duan, Z., et al. (2021). SARS-CoV-2 envelope protein causes acute respiratory distress syndrome (ARDS)-like pathological damages and constitutes an antiviral target. Cell Res. *31*, 847–860. https://doi.org/10.1038/s41422-021-00519-4.
45. Khan, S., Shafiei, M.S., Longoria, C., Schoggins, J.W., Savani, R.C., and Zaki, H. (2021). SARS-CoV-2 spike protein induces inflammation via TLR2-dependent activation of the NF-kappaB pathway. Elife *10*, e68563. https://doi.org/10.7554/eLife.68563.
46. Kim, M.J., Kim, J.Y., Shin, J.H., Son, J., Kang, Y., Jeong, S.K., Kim, D.H., Kim, K.H., Chun, E., and Lee, K.Y. (2024). The SARS-CoV-2 spike protein induces lung cancer migration and invasion in a TLR2-dependent manner. Cancer Commun. *44*, 273–277. https://doi.org/10.1002/cac2.12485.
47. Petruk, G., Puthia, M., Petrlova, J., Samsudin, F., Strömdahl, A.C., Cerps, S., Uller, L., Kjellström, S., Bond, P.J., and Schmidtchen, A.A. (2020). SARS-CoV-2 spike protein binds to bacterial lipopolysaccharide and boosts proinflammatory activity. J. Mol. Cell Biol. *12*, 916–932. https://doi.org/10.1093/jmcb/mjaa067.
48. Tang, Z., Xu, Y., Tan, Y., Shi, H., Jin, P., Li, Y., Teng, J., Liu, H., Pan, H., Hu, Q., et al. (2023). CD36 mediates SARS-CoV-2-envelope-protein-induced platelet activation and thrombosis. Nat. Commun. *14*, 5077. https://doi.org/10.1038/s41467-023-40824-7.
49. Ewart, G., Bobardt, M., Bentzen, B.H., Yan, Y., Thomson, A., Klumpp, K., Becker, S., Rosenkilde, M.M., Miller, M., and Gallay, P. (2023). Post-infection treatment with the E protein inhibitor BIT225 reduces disease severity and increases survival of K18-hACE2 transgenic mice infected with a lethal dose of SARS-CoV-2. PLoS Pathog. *19*, e1011328. https://doi.org/10.1371/journal.ppat.1011328.
50. Raschetti, R., Vivanti, A.J., Vauloup-Fellous, C., Loi, B., Benachi, A., and De Luca, D. (2020). Synthesis and systematic review of reported neonatal SARS-CoV-2 infections. Nat. Commun. *11*, 5164. https://doi.org/10.1038/s41467-020-18982-9.
51. Barrero-Castillero, A., Beam, K.S., Bernardini, L.B., Ramos, E.G.C., Davenport, P.E., Duncan, A.R., Fraiman, Y.S., Frazer, L.C., Healy, H., Herzberg, E.M., et al. (2021). COVID-19: neonatal-perinatal perspectives. J. Perinatol. *41*, 940–951. https://doi.org/10.1038/s41372-020-00874-x.
52. Precit, M.R., Yee, R., Anand, V., Mongkolrattanothai, K., Pandey, U., and Dien Bard, J. (2020). A Case Report of Neonatal Acute Respiratory Failure Due to Severe Acute Respiratory Syndrome Coronavirus-2. J. Pediatric Infect. Dis. Soc. *9*, 390–392. https://doi.org/10.1093/jpids/piaa064.
53. Consiglio, C.R., Cotugno, N., Sardh, F., Pou, C., Amodio, D., Rodriguez, L., Tan, Z., Zicari, S., Ruggiero, A., Pascucci, G.R., et al. (2020). The Immunology of Multisystem Inflammatory Syndrome in Children with COVID-19. Cell *183*, 968–981.e7. https://doi.org/10.1016/j.cell.2020.09.016.
54. Li, Y., Schneider, A.M., Mehta, A., Sade-Feldman, M., Kays, K.R., Gentili, M., Charland, N.C., Gonye, A.L., Gushterova, I., Khanna, H.K., et al. (2021). SARS-CoV-2 viremia is associated with distinct proteomic pathways and predicts COVID-19 outcomes. J. Clin. Invest. *131*, e148635. https://doi.org/10.1172/JCI148635.
55. Fajnzylber, J., Regan, J., Coxen, K., Corry, H., Wong, C., Rosenthal, A., Worrall, D., Giguel, F., Piechocka-Trocha, A., Atyeo, C., et al. (2020). SARS-CoV-2 viral load is associated with increased disease severity and mortality. Nat. Commun. *11*, 5493. https://doi.org/10.1038/s41467-020-19057-5.
56. Loftus, T.J., Ungaro, R., Dirain, M., Efron, P.A., Mazer, M.B., Remy, K.E., Hotchkiss, R.S., Zhong, L., Bacher, R., Starostik, P., et al. (2021). Overlapping but Disparate Inflammatory and Immunosuppressive Responses to SARS-CoV-2 and Bacterial Sepsis: An Immunological Time Course Analysis. Front. Immunol. *12*, 792448. https://doi.org/10.3389/fimmu.2021.792448.
57. Yalcinkaya, M., Liu, W., Islam, M.N., Kotini, A.G., Gusarova, G.A., Fidler, T.P., Papapetrou, E.P., Bhattacharya, J., Wang, N., and Tall, A.R. (2021). Modulation of the NLRP3 inflammasome by Sars-CoV-2 Envelope protein. Sci. Rep. *11*, 24432. https://doi.org/10.1038/s41598-021-04133-7.
58. Nedeva, C., Menassa, J., and Puthalakath, H. (2019). Sepsis: Inflammation Is a Necessary Evil. Front. Cell Dev. Biol. *7*, 108. https://doi.org/10.3389/fcell.2019.00108.
59. Nakamori, Y., Park, E.J., and Shimaoka, M. (2020). Immune Deregulation in Sepsis and Septic Shock: Reversing Immune Paralysis by Targeting PD-1/PD-L1 Pathway. Front. Immunol. *11*, 624279. https://doi.org/10.3389/fimmu.2020.624279.
60. Cavaillon, J.M., and Adib-Conquy, M. (2006). Bench-to-bedside review: endotoxin tolerance as a model of leukocyte reprogramming in sepsis. Crit. Care *10*, 233. https://doi.org/10.1186/cc5055.
61. Liu, D., Cao, S., Zhou, Y., and Xiong, Y. (2019). Recent advances in endotoxin tolerance. J. Cell. Biochem. *120*, 56–70. https://doi.org/10.1002/jcb.27547.
62. Lee, M.J., Bae, J., Lee, J.H., Park, Y.J., Lee, H.A.R., Mun, S., Kim, Y.S., Yune, C.J., Chung, T.N., and Kim, K. (2022). Serial Change of Endotoxin Tolerance in a Polymicrobial Sepsis Model. Int. J. Mol. Sci. *23*, 6581. https://doi.org/10.3390/ijms23126581.
63. Arens, C., Bajwa, S.A., Koch, C., Siegler, B.H., Schneck, E., Hecker, A., Weiterer, S., Lichtenstern, C., Weigand, M.A., and Uhle, F. (2016). Sepsis-induced long-term immune paralysis–results of a descriptive, explorative study. Crit. Care *20*, 93. https://doi.org/10.1186/s13054-016-1233-5.
64. Liu, J., Qian, C., and Cao, X. (2016). Post-Translational Modification Control of Innate Immunity. Immunity *45*, 15–30. https://doi.org/10.1016/j.immuni.2016.06.020.

65. Perkins, D.J., Patel, M.C., Blanco, J.C.G., and Vogel, S.N. (2016). Epigenetic Mechanisms Governing Innate Inflammatory Responses. J. Interferon Cytokine Res. *36*, 454–461. https://doi.org/10.1089/jir.2016.0003.
66. Mussbacher, M., Derler, M., Basílio, J., and Schmid, J.A. (2023). NF-kappaB in monocytes and macrophages - an inflammatory master regulator in multitalented immune cells. Front. Immunol. *14*, 1134661. https://doi.org/10.3389/fimmu.2023.1134661.
67. Porta, C., Rimoldi, M., Raes, G., Brys, L., Ghezzi, P., Di Liberto, D., Dieli, F., Ghisletti, S., Natoli, G., De Baetselier, P., et al. (2009). Tolerance and M2 (alternative) macrophage polarization are related processes orchestrated by p50 nuclear factor kappaB. Proc. Natl. Acad. Sci. USA *106*, 14978–14983. https://doi.org/10.1073/pnas.0809784106.
68. Liu, J., Xiang, J., Li, X., Blankson, S., Zhao, S., Cai, J., Jiang, Y., Redmond, H.P., and Wang, J.H. (2017). NF-kappaB activation is critical for bacterial lipoprotein tolerance-enhanced bactericidal activity in macrophages during microbial infection. Sci. Rep. *7*, 40418. https://doi.org/10.1038/srep40418.
69. Pello, O.M., De Pizzol, M., Mirolo, M., Soucek, L., Zammataro, L., Amabile, A., Doni, A., Nebuloni, M., Swigart, L.B., Evan, G.I., et al. (2012). Role of c-MYC in alternative activation of human macrophages and tumor-associated macrophage biology. Blood *119*, 411–421. https://doi.org/10.1182/blood-2011-02-339911.
70. Deshpande, R., Li, W., Li, T., Fanning, K.V., Clemens, Z., Nyunoya, T., Zhang, L., Deslouches, B., Barchowsky, A., Wenzel, S., et al. (2024). SARS-CoV-2 Accessory Protein Orf7b Induces Lung Injury via c-Myc Mediated Apoptosis and Ferroptosis. Int. J. Mol. Sci. *25*, 1157. https://doi.org/10.3390/ijms25021157.
71. Schneider, C.A., Rasband, W.S., and Eliceiri, K.W. (2012). NIH Image to ImageJ: 25 years of image analysis. Nat. Methods *9*, 671–675. https://doi.org/10.1038/nmeth.2089.
72. Brown, J., Pirrung, M., and McCue, L.A. (2017). FQC Dashboard: integrates FastQC results into a web-based, interactive, and extensible FASTQ quality control tool. Bioinformatics *33*, 3137–3139. https://doi.org/10.1093/bioinformatics/btx373.
73. Dobin, A., Davis, C.A., Schlesinger, F., Drenkow, J., Zaleski, C., Jha, S., Batut, P., Chaisson, M., and Gingeras, T.R. (2013). STAR: ultrafast universal RNA-seq aligner. Bioinformatics *29*, 15–21. https://doi.org/10.1093/bioinformatics/bts635.
74. Anders, S., Pyl, P.T., and Huber, W. (2015). HTSeq–a Python framework to work with high-throughput sequencing data. Bioinformatics *31*, 166–169. https://doi.org/10.1093/bioinformatics/btu638.
75. Love, M.I., Huber, W., and Anders, S. (2014). Moderated estimation of fold change and dispersion for RNA-seq data with DESeq2. Genome Biol. *15*, 550. https://doi.org/10.1186/s13059-014-0550-8.
76. Subramanian, A., Tamayo, P., Mootha, V.K., Mukherjee, S., Ebert, B.L., Gillette, M.A., Paulovich, A., Pomeroy, S.L., Golub, T.R., Lander, E.S., and Mesirov, J.P. (2005). Gene set enrichment analysis: a knowledge-based approach for interpreting genome-wide expression profiles. Proc. Natl. Acad. Sci. USA *102*, 15545–15550. https://doi.org/10.1073/pnas.0506580102.

## STAR★METHODS

### KEY RESOURCES TABLE

| REAGENT or RESOURCE | SOURCE | IDENTIFIER |
|---|---|---|
| Antibodies | | |
| mouse anti-TLR2 | Santa Cruz Biotechnology | MA5-16200; RRID:AB_2537718 |
| rabbit anti-TLR4 | Abcam | ab13556; RRID:AB_300457 |
| mouse anti-ICAM1 | Santa Cruz Biotechnology | sc-8439; RRID:AB_627123 |
| mouse anti-β-Actin | Sigma Aldrich | A1978; RRID:AB_476692 |
| rabbit anti-P38 | Cell Signaling Technologies | 8690; RRID:AB_10999090 |
| rabbit anti-Phospho-P38 (Thr180/Tyr182) | Cell Signaling Technologies | 4511; RRID:AB_2139682 |
| rabbit anti-P65 | Cell Signaling Technologies | 8242; RRID:AB_10859369 |
| Rabbit anti-Phospho-P65 | Cell Signaling Technologies | 3033; RRID:AB_331284 |
| Biological samples | | |
| Deidentified healthy PBMC biospecimens | StemCell Technologies | 70025.2 |
| Chemicals, peptides, and recombinant proteins | | |
| Forget-Me-Not™ EvaGreen® qPCR Master Mix | Biotium | 31041 |
| Recombinant SARS-CoV-2 Envelope protein | Novus Biologicals | NBP2-90986 |
| Recombinant SARS-CoV-2 Envelope Protein | AbClonal | RP01263LQ |
| Luna Script | New England Bio Labs | E3010L |
| TRIzol reagent | Thermo Fisher Scientific | 15596018 |
| Recombinant SARS-CoV-2 spike protein | Sino Biological | 40589-V08B1 |
| Recombinant SARS-CoV-2 nucleocapsid protein | Sino Biological | 40588-V08B |
| LPS | InvivoGen | tlrl-peklps |
| HEK-Blue selection reagent | InvivoGen | hb-sel |
| HEK-Blue detection medium | InvivoGen | hb-det2 |
| Heat killed-Listeria | InvivoGen | tlrl-hklm |
| QUANTI-Luc reagent | InvivoGen | rep-qlc4lg1 |
| QUANTI-Blue solution | InvivoGen | rep-qbs1 |
| Critical commercial assays | | |
| Rneasy Micro Kit | Qiagen | 74034 |
| Qubit RNA High Sensitivity kit | Thermo Fisher Scientific | Q32852 |
| TruSeq Stranded Total RNA Library Prep Human/Mouse/Rat Kit | Illumina | 20020596 |
| EasySep Human Monocyte Isolation Kit | StemCell Technologies | 19669 |
| Cytokine 25-plex Human Panel kit | Thermo Fisher Scientific | LHC0009M |
| Deposited data | | |
| RNA-seq of monocytes | NIH SRA database | BioProject ID PRJNA1029483 |
| Experimental models: Cell lines | | |
| HEK-Blue (HEK 293) cells overexpressing hTLR2 | InvivoGen | hkb-htlr2 |
| HEK-Blue (HEK 293) cells overexpressing hTLR4 | InvivoGen | hkb-htlr4 |
| THP1-Dual monocyte cell lines | InvivoGen | thpd-nfis |
| THP1-Dual KO-TLR2 monocyte cell lines | InvivoGen | thpd-kotlr2 |
| Experimental models: Organisms/strains | | |
| C57BL6 mice | Charles River | C57BL/6NCrl |

(*Continued on next page*)

*Continued*

| REAGENT or RESOURCE | SOURCE | IDENTIFIER |
|---|---|---|
| Oligonucleotides | | |
| KiCqStart SYBR primers (Il-1β, Tnf-α, Ifn-α, and 18s rRNA) | Sigma Aldrich | N/A |
| Software and algorithms | | |
| GraphPad Prism (version 10) | GraphPad | Version 10 |
| ImageJ Software | Schneider et al.[71] | https://imagej.nih.gov/ij/ |
| FastQC | Brown et al.[72] | https://www.bioinformatics.babraham.ac.uk/projects/fastqc/ |
| STAR | Dobin et al.[73] | https://github.com/alexdobin/STAR/releases |
| htseq-count | Anders et al.[74] | https://pypi.org/project/HTSeq/ |
| R package DESeq2 | Love et al.[75] | https://www.bioconductor.org/packages/release/bioc/html/DESeq2.html |
| GSEA | Subramanian et al.[76] | https://www.gsea-msigdb.org/gsea/index.jsp |
| ProcartaPlex Analysis App | Thermo Fisher Scientific | https://www.thermofisher.com/us/en/home/life-science/antibodies/immunoassays/procartaplex-assays-luminex/procartaplex-immunoassays/procartaplex-analyst-software.html |

## RESOURCE AVAILABILITY

### Lead contact

Further information and requests for resources and reagents should be directed to and will be fulfilled by the lead contact, Todd Bradley (tcbradley@cmh.edu).

### Materials availability

This study did not generate new unique reagents.

### Data and code availability

#### *Data availability*

The data that support the findings of this study are available from the corresponding author, T.B., upon reasonable request. The primary data from the RNA-seq of monocytes is deposited in the NIH SRA database under BioProject ID PRJNA1029483 (SRA: PRJNA1029483). Data reported in this paper will be shared by the lead contact upon request.

#### *Code availability*

This paper does not report original code. Any additional information required to reanalyze the data reported in this paper is available from the lead contact upon request.

## EXPERIMENTAL MODEL AND STUDY PARTICIPANT DETAILS

### Human subjects

Deidentified healthy PBMC biospecimens were obtained through StemCell Technologies and were obtained in compliance with applicable federal, state, and local laws, regulations, and guidance using Informed Consent Forms and protocols approved by either an Institutional Review Board, the Food and Drug Administration (FDA), the U.S. Department of Health and Human Services, and/or an equivalent regulatory authority. The specimens used for study consisted of six females and seven males with ages ranging from 21 to 60 (median 29 years old) years old. 12 of the 13 individuals were Caucasian and one individual had Hispanic ethnicity. No other demographic or clinical information is available from these deidentified specimens. This study did not determine the association of age, sex and ethnicity on the experimental outcomes.

### Mice

The mice used in the experimental procedures were cared for in accordance with the guidelines set forth by the University of Missouri-Kansas City Lab Animal Resource Center and the National Institutes of Health's regulations for the care and use of laboratory animals. All protocols were approved in advance by the University of Missouri-Kansas City Institutional Animal Care and Use Committee, protocol number 41066.

The C57BL6 mouse strain was obtained from Charles River (Stillwell, KS, USA). At postnatal day 5, sex is unable to be determined, thus the sex of the mice used in the study are unknown. This study did not determine the association of sex on the outcomes.

## METHOD DETAILS

### Monocyte isolation and culture

Cryopreserved vials of PBMCs, unique donors, were acquired (StemCell Technologies, Vancouver, BC, Canada), thawed according to manufacturer guidelines and resuspended in phosphate buffered saline (PBS) with 0.1% bovine serum albumin (BSA) and counted on the Countess III (Thermo Fisher Scientific, Waltham, MA, USA). Monocytes were then isolated from PBMC using the EasySep Human Monocyte Isolation Kit (StemCell Technologies) following manufacturer guidelines. Isolated monocytes were resuspended in 1 mL of RPMI-1640 (Thermo Fisher Scientific) with 10% fetal bovine serum (FBS; Thermo Fisher Scientific), referred to as complete media. On day 0, monocytes were plated at 500,000 cells in each well of a 12 well plate (1 mL total complete media each well) and incubated for 16–18 h overnight at 37°C, 5% $CO_2$. On day 1, depending on the experiment, monocytes were stimulated with 1 μg/mL, 10 ng/mL, 1 ng/mL or 10 pg/mL of recombinant SARS-CoV-2 envelope protein (Novus Biologicals, Centennial, CO, USA), 1 μg/mL of SARS-CoV-2 spike recombinant protein (Sino Biological, Wayne, PA, USA) or 1 μg/mL of nucleocapsid protein (Sino Biological) for 24 h. On day 2, the media from each well was transferred to a microcentrifuge tube and centrifuged at 300 g for 10 min at room temperature. Supernatant was transferred to a new tube without disturbing the cell pellet and stored at −80°C for multiparameter immunoassays. Monocyte pellets were resuspended and washed once in 1 mL of PBS, recentrifuged for 300 g for 10 min, resuspended in 1 mL of complete media and incubated until day 6, with one media change on day 4. On Day 6, media was changed, and cells were given a secondary stimulation of 1 μg/mL LPS (InvivoGen, San Diego, CA, USA) or 1 ug/mL of SARS-CoV-2 envelope protein (Novus Biologicals). Control samples were not given any primary stimulation on day 1 but did receive the secondary LPS stimulation on day 6. Baseline samples received no stimulations during the experiment. On day 7, cells were centrifuged (300 g for 10 min) and supernatant was harvested and frozen at −80°C for multiparameter immunoassays.

### Luminex multiplexed cytokine and chemokine measurements

Cell culture supernatants from days 2 and 7 were thawed on ice, and then centrifuged at 16000 g for 10 min. For secreted analyte quantification, supernatants were analyzed using the Cytokine 25-plex Human Panel kit (Thermo Fisher Scientific) and analyzed on the Luminex Magpix Multiplexing system using manufacturer recommended instrument settings (Luminex Corporation, Austin, TX, USA). This kit measures the concentration of 25 different cytokines, chemokines, and growth factors critical for monocyte inflammatory function. Raw instrument data and validated standard concentration curves for each of the 25 analytes were exported and analyzed using the Thermo Fisher Scientific ProcartaPlex Analysis App for immunoassays (https://www.thermofisher.com/us/en/home/life-science/antibodies/immunoassays/procartaplex-assays-luminex/procartaplex-immunoassays/procartaplex-analyst-software.html). Any analyte standards with concentrations that varied more than 120% or less than 80% of their expected concentration were removed from analysis. After standard curve validation, any analytes that were under the lower quantitative range for each of the tested conditions, defined as the concentration of the lowest standard for each analyte, were removed.

### SARS-CoV-2 E and S protein stimulation of TLR2 and TLR4 overexpressing HEK cells

HEK-Blue (HEK 293) cells overexpressing hTLR2 or hTLR4 (InvivoGen). Cells were thawed and maintained in growth medium (DMEM 10% FBS, 4.5 g/L glucose, 2 mM glutamine, 100 units/mL Pen-Strep and 100 μg/mL normocin) supplemented with 1x HEK-Blue selection reagent (InvivoGen) and maintained according to manufacturer culturing guidelines. Prior to E and S protein stimulation, HEK-TLR2 and HEK-TLR4 cells were resuspended in HEK-Blue detection medium (InvivoGen) at 50,000 cells per well in a 96 well plate. E protein and S protein aliquots were added to wells for final working concentrations of 4, 2, 1, 0.5 and 0.25 μg/mL of either E protein or S protein. For a positive control of hTLR2 activation, TLR2 agonist Heat killed-Listeria (InvivoGen) at a concentration of 10^9 cells/mL was used. For a positive control of hTLR4 activation, 1 μg/mL of TLR 4 agonist LPS (InvivoGen) was used. Endotoxin-free water was used as a negative control for both TLR2 and TLR4. Cells were incubated with these stimuli for 16 h and then TLR2 or TLR4 activation was measured on a plate reader measuring Optical Density (620-655 nm) of secreted alkaline phosphatase, a reporter gene used to measure NF-κB activation for both the hTLR2 and hTLR4 cells.

### SARS-CoV-2 E protein stimulation of THP-1 and THP-1 TLR2 knockout cells

THP1-Dual (InvivoGen) and THP1-Dual KO-TLR2 (InvivoGen) monocyte cell lines contain stable integration of two reporter genes within the IRF pathway. Lucia luciferase, a secreted luciferase reporter gene, under control of an ISG54 minimal promoter, and a secreted embryonic alkaline phosphatase (SEAP) reporter gene driven by an IFN-β minimal promoter. Cells were grown in RPMI 1640 growth media (10% FBS, 2 mM glutamine, Pen-Strep (100 Units/mL-100 μg/mL), 50 mg/mL normocin, 10 mg/mL Blasticidin, 100 mg/mL Zeocin) and maintained according to manufacturer culturing guidelines. 50,000 cells per well were seeded into a 96 well plate in technical triplicate. Cells were treated with either media or SARS-CoV-2 Envelope Protein (Novus Biologicals) at 1:2 titrated concentrations ranging from 4 μg/mL to 250 ng/mL for 16 h hTLR2, TLR2 agonist Heat killed-Listeria (InvivoGen), was used as a TLR2 positive control at a concentration of 10^9 cells/mL was used. hTLR4, TLR4 agonist LPS (InvivoGen), was used as a TLR4 positive control at a concentration of 1 μg/mL. For luciferase reporting, 20 μL of supernatant was added to 50 μL of 1X QUANTI-Luc reagent (InvivoGen) in a white walled 96 well plate. Luminescence was read immediately

with a 0.1 s reading time on a microplate reader. For SEAP reporting, 20 μL of supernatant was added to 180 μL of QUANTI-Blue solution (InvivoGen) in a 96 well plate and incubated at 37°C for 1 h. Absorbance of the plate was read at 630 nM using microplate reader.

For experiments where THP-1 cells were treated with primary stimulation, rested then secondary stimulation the THP1-Dual and THP1-Dual KO-TLR2 cell lines were treated with either media or 1 μg/mL of SARS-CoV-2 Envelope protein for 16 h in technical triplicate in a V-bottom 96 well plate. Cells were centrifuged, media was removed, and washed with fresh media twice to remove remaining E protein. Cells were resuspended with fresh media and let rest for 5 days. On day 5, media was removed, and cells were washed once more prior to cells being treated with 1 μg/mL of LPS for 16 h. Luciferase and SEAP reporters were measured as described above to measure cell activation levels.

### RNA-sequencing of human monocytes

Monocytes were isolated from cryopreserved PBMC from three individual healthy donors and plated as already described. On day 1, monocytes were given either PBS ($n$ = 3; control), 1 μg/mL SARS-CoV-2 E protein ($n$ = 3; Novus Biologicals) and incubated for 24 h. On day 2, media was changed, and cells were incubated until day 6 as described above. On day 6, monocytes were harvested and processed for RNA extraction using the Rneasy Micro Kit from (Qiagen, Germantown, MD, USA). RNA concentrations were determined using the Qubit RNA High Sensitivity kit on a Qubit fluorometer (Thermo Fisher Scientific). RNA libraries were prepared with the TruSeq Stranded Total RNA Library Prep Human/Mouse/Rat Kit (Illumina, San Diego, CA, USA). Libraries were run on the Illumina Nova-Seq 6000 in the 2 × 151 bp paired-end format. After sequencing, initial quality check for library complexity and per-base sequence quality throughout all reads was done using FastQC (v0.11.7) software. Next, trimming of low-quality bases (<20), short reads (<30), and adaptor sequences was done with the fastqc-mcf (v1.05). Reads were then aligned to GRCh38/hg38 using STAR (v2.7). htseq-count (v0.6.0) was used to generate the counts table for the features. Differential gene expression analysis was carried out using R package DESeq2 (v1.26.0). GSEA v4.1.0 was used for gene set enrichment analysis. Raw counts matrix obtained after running htseq-count were normalized using DESeq2 to generate expression dataset. Next, phenotype file was prepared based on group information for the samples. Hallmark gene sets (v7.4) and Human_HGNV_ID_MiSigDB (v7.4) chip hosted on the GSEA-MsigDB file servers were used as Gene sets and Chip annotation file respectively. Genes weren't collapsed and "gene_set" parameter was used for permutation. While rest of the options were run with default settings.

### Mouse immunization with SARS-CoV-2 E protein

Mice (P5) were i.p. injected with the 2 mg/kg of E protein (Abclonal, Woburn, MA) or sterile saline. This was followed by subsequent i.p. injection of LPS (2 mg/kg). The pups were left with the dam and closely monitored for signs of distress after treatments. Pups were euthanized on P14 using a 100 mg/kg ip pentobarbital injection, exsanguinated after cessation of heartbeat, and lungs were harvested. For all experiments, a minimum of 4 or 5 mice/group were used.

### Quantification of mRNA expression using real-time PCR

RNA was extracted on day 9 of experiment from 14-day old mouse lung homogenates using the TRIzol reagent (Thermo Fisher Scientific). cDNA was synthesized from 1 μg of RNA using Luna Script (New England Bio Labs, Ipswich, MA, USA) according to the manufacturers protocol. Real-time PCR was performed using a Forget-Me-Not EvaGreen qPCR Master Mix (Biotium, Fremont, CA, USA). 18S rRNA expression was used to normalize qRT-PCR values across different experiments with relative gene expression calculated using the Pflaffl method. The following primers were purchased pre-validated from Sigma's KiCqStart SYBR primers (Sigma Aldrich, St Louis, MO, USA): Il-1β, Tnf-α, Ifn-α, and 18s rRNA.

### Immunoblotting for quantifying changes in protein expression

Mouse lung tissue from 14-day old mice, day 9 of experiment, were homogenized in RIPA lysis buffer containing protease and phosphatase inhibitors (Sigma Aldrich), with the clarified protein lysates used for Western blotting. Immunoblotting was done following standard protocol. Primary antibodies used were: Rabbit anti-Phospho-P65 (Ser536, Cell Signaling Technologies (CST), Danvers, MA), rabbit anti-P65 (CST), rabbit anti-Phospho-P38 (Thr180/Tyr182, CST), rabbit anti-P38 (CST), mouse anti-β-Actin (Sigma Aldrich), mouse anti-ICAM1 (Santa Cruz Biotechnology, Dallas, TX, USA), rabbit anti-TLR4 (Abcam, Waltham, MA USA) and mouse anti-TLR2 (Santa Cruz Biotechnology). Densitometry was done using ImageJ Software (NIH, Bethesda, MD, USA) and changes were normalized to β-Actin or the corresponding non-phosphorylated antibody.

## QUANTIFICATION AND STATISTICAL ANALYSIS

To determine statistical differences in concentrations of specific analytes nonparametric paired or unpaired (depending on the comparison) Wilcoxon-Mann-Whitney test was performed. For the mouse study, a minimum of 4 mice per group was used. RNA quantification and PCR results were based on two to three technical replicates. Prior to conducting statistical analysis, we assessed whether the data distribution was Gaussian using the D'Agostino–Pearson omnibus normality test. If the data were normally distributed, ANOVA with a post-hoc Tukey test was used for analysis. If the data did not meet Gaussian assumptions, a Mann–Whitney U test was used for analysis. In most cases, fold changes were calculated relative to expression/changes in untreated controls. Statistical analysis was carried out using GraphPad Prism (version 10).